

Non-invasive assessment of ventriculo-arterial coupling using aortic wave intensity analysis combining central blood pressure and phase-contrast cardiovascular magnetic resonance

Bhuva AN^{1,2}, D'Silva A³, Torlasco C⁴, Nadarajan N¹, Jones S¹, Boubertakh R², Van Zalen J², Scully P^{1,2}, Knott K^{1,2}, Benedetti G², Augusto JB^{1,2}, Rachel Bastiaenen³, Lloyd G², Sharma S³, Moon JC^{1,2}, Parker KH⁵, Manisty CH^{1,2}, Hughes AD^{1,6}

1. Institute of Cardiovascular Science, University College London, UK
2. Barts Heart Centre, London, UK
3. Cardiovascular Sciences Research Centre, St. George's, University of London, London, United Kingdom
4. IRCCS, Istituto Auxologico Italiano, Milan, Italy
5. Department of Bioengineering, Imperial College London, UK
6. MRC Unit for Lifelong Health and Ageing at UCL, London, UK

Correspondence:

Dr Alun D Hughes
69 Chenies Mews
Institute of Cardiovascular Sciences
University College London
WC1E6HX
Telephone: 0207 679 9525
Fax: 0207 580 1501

Running title: Wave intensity analysis using CMR and central BP.

Keywords: wave intensity analysis; ventriculo-arterial coupling; reflection index; hemodynamics; CMR; aorta

Financial support: The Marathon Study was funded by the British Heart Foundation (FS/15/27/31465), Cardiac Risk in the Young, and the Barts Cardiovascular Biomedical Research Centre. AB is supported by a doctoral research fellowship from the British Heart Foundation (FS/16/46/32187). AH received support from the British Heart Foundation (PG/13/6/29934), the National Institute for Health Research University College London Hospitals Biomedical Research Centre, and works in a unit that receives support from the UK Medical Research Council (MC_UU_12019/1). AD and PS were funded by clinical research training fellowships from the British Heart Foundation, United Kingdom (FS/15/27/31465 and FS/16/31/32185). JCM and CM are directly and indirectly supported by the University College London Hospitals, NIHR Biomedical Research Centre and Biomedical Research Unit at Barts Hospital, respectively.

Disclosures: None.

Abstract

Background Wave intensity analysis (WIA) in the aorta offers important clinical and mechanistic insight into ventriculo-arterial coupling, but is difficult to measure non-invasively. We performed WIA by combining standard cardiovascular magnetic resonance (CMR) flow-velocity and non-invasive central blood pressure (BP) waveforms.

Methods and Results 206 healthy volunteers (age range 21- 73 years, 47% male) underwent sequential phase contrast CMR (Siemens Aera 1.5T, $1.97 \times 1.77\text{mm}^2$, 9.2ms temporal resolution) and supra-systolic oscillometric central BP measurement (200Hz). Velocity (U) and central pressure (P) waveforms were aligned using the waveform foot, and local wave speed was calculated both from the PU-loop (c) and the sum of squares method (c_{SS}). These were compared with CMR transit time derived aortic arch pulse wave velocity (PWV_{tt}). Associations were examined using multivariable regression.

The peak intensity of the initial compression wave, backward compression wave and forward decompression wave were 69.5 ± 28 , -6.6 ± 4.2 and $6.2 \pm 2.5 \times 10^4 \text{ W/m}^2/\text{cycle}^2$ respectively; reflection index was 0.10 ± 0.06 . PWV_{tt} correlated with c or c_{SS} ($r = 0.60$, and 0.68 respectively, $p < 0.01$ for both). Increasing age decade and female sex were independently associated with decreased forward compression wave (-8.6 and $-20.7 \text{ W/m}^2/\text{cycle}^2$ respectively, $p < 0.01$) and greater wave reflection index (0.02 and 0.03 respectively, $p < 0.001$).

Conclusion This novel non-invasive technique permits straightforward measurement of wave intensity at scale. Local wave speed showed good agreement with PWV_{tt} , and correlation was stronger using the sum of squares method than the PU-loop. Ageing and female sex were associated with poorer ventriculo-arterial coupling in healthy individuals.

Abbreviations

BCW	Backward compression wave
BP	Blood pressure
BSA	Body-surface area
c	Local wave speed estimated from pressure-velocity loop
CMR	Cardiovascular magnetic resonance imaging
cSS	Local wave speed estimated from sum of squares method
FCW	Forward compression wave
FDW	Forward (protodiastolic)decompression wave
HR	Heart rate
MAP	Mean arterial pressure
P	Pressure
PWV_{tt}	Pulse wave velocity calculated using transit time
U	Velocity
WIA	Wave intensity analysis

Introduction

An integrated assessment of the cardiovascular system is clinically and mechanistically important, yet ventricular and arterial function are often considered in isolation. Wave intensity analysis (WIA) is a technique that characterizes flow generated by the heart and the afterload imposed by the vasculature in terms of wave propagation. (1,2) It also calculates wave reflection and wave speed which predict coronary and cardiac events, independently of conventional cardiovascular risk factors.(3–8)

Waves transmit energy and arise in the circulation as a result of cardiac contraction and relaxation or reflection. Because reflection occurs from circulatory sites of impedance mismatching, WIA describes the efficiency of energy transfer in the cardiovascular system. The magnitude of energy transferred by a wave is quantified as the product of changing pressure and flow-velocity at the same location.(9) Waves are further characterized by their direction of travel (forwards or backwards), and the pressure gradient across them (compression or decompression waves). Both these characteristics determine their impact on pressure and flow (e.g. a forward compression wave increases pressure and accelerates flow whereas a forward decompression decreases pressure and decelerates flow). In addition to measuring the timing and intensity of waves, WIA can quantify local wave speed, a measure of arterial stiffness.(9–12) The relationship with the reference standard of regional pulse wave velocity measured from transit time (PWV_{tt}) has not been established.

Traditionally, WIA has been derived invasively using simultaneous catheter measures of pressure and flow or velocity.(13) It has offered insights into a range of diseases but because of feasibility, understanding of healthy ageing and sex differences in the aorta has been limited.(14–17) Phase-contrast cardiovascular magnetic resonance imaging (CMR) allows non-invasive assessment of aortic flow, and CMR is the gold-standard for anatomically standardized cross-sectional measurements. CMR distensibility has successfully been used as

a central pressure surrogate to perform WIA, but the method does not provide a direct measure of wave energy and can be technically challenging.(14,18) Cuff based devices simplify the acquisition of central blood pressure waveform data and show good agreement with invasive measures.(19)

The aims of this study were (1) to use non-invasive direct measures of the central blood pressure (cBP) and velocity waveforms to perform wave intensity analysis, (2) to compare measures of local wave speed with a reference of conventionally calculated PWV_{tt} , and (3) to evaluate associations between aortic WIA and age and sex in healthy individuals.

Methods

Study population

237 healthy participants were recruited from the pre-training assessment of the Marathon Study. This is an observational study recruiting healthy volunteers to investigate the effects of first-time marathon training on cardiovascular function.(20) Acquisition of data for WIA did not add extra time to the standard tests performed. Inclusion criteria were: age over 18 years, no past significant medical history, no previous marathon-running experience, and current participation in running for <2 hours per week. All procedures were in accordance with the principles of the Helsinki declaration, all participants gave written informed consent and the study was approved by the London Queen Square National Research Ethics Service Committee (15/LO/0086).

A total of 211 participants underwent paired phase-contrast CMR and central blood pressure waveform recording (Supplemental Figure 1). Five participants were excluded due to noisy blood pressure profiles, leaving a total 206 participants.

Central blood pressure and heart rate estimation

Supra-systolic oscillometric brachial blood pressure was measured over ten seconds with a sampling frequency of 200Hz in duplicate after a period of rest in the semi-supine position. (Cardioscope II BP+, Uscom Ltd, Sydney, Australia). A single ensemble averaged central pressure estimate (*P*) was derived from the second ten-second measurement of the brachial supra-systolic arterial waveforms, as previously described.(21) This has been shown to yield highly correlated central systolic BPs and pressure waveforms with invasive catheter assessment, no bias, and good intra-and re-test reliability .(21,22) Heart rate (HR) was taken as the average of the HR during the recording.

CMR acquisition and analysis

After BP acquisition, CMR was performed at 1.5T (Magnetom Aera, Siemens AG Healthcare, Erlangen, Germany). Participants were supine for approximately half an hour of scanning before the sequence acquisitions used for this analysis. Single-shot ECG-gated white blood sagittal aortic ('candy cane') views were acquired first, to allow 3D aortic arch length measurement and standardized cross-sectional imaging. This was used to pilot axial aortic blood flow-velocity maps at the level of the pulmonary artery bifurcation. The spoiled gradient echo phase-contrast sequence used was free-breathing, ECG-gated and segmented, with the following parameters: acquired temporal resolution 9.2ms (reconstructed to 100 cardiac phases per RR interval); spatial resolution 1.97 x 1.77 mm²; slice thickness 6mm; through-plane velocity encoding 150cm/s; field of view 192 x 108mm; flip angle 20°. Images were analyzed using validated software to obtain velocity-time profiles for the ascending and descending aorta (ArtFun, University Pierre Marie Curie–INSERM).(23,24) The only user interaction was to select the center and border of the lumen on the modulus imaging. A circular cross-sectional aortic lumen region of interest (ROI) was then contoured automatically and propagated to each velocity-encoded phase; automatic contours were checked and modified manually if necessary. Mean aortic velocity within each ROI was then calculated for every phase to plot a velocity-time profile. Ascending aortic velocity-time profiles (*U*) were combined with BP waveforms for WIA (**Figure 1**). **Figure 2** provides a flow chart of data acquisition and analysis.

Pulse wave velocity (PWV_{tt}) calculation using transit time

Aortic arch PWV was calculated from the 3D distance between the ascending and descending aortic locations of the phase-contrast imaging and the transit time between velocity profiles:

$$Aortic\ arch\ PWV_{tt}(cm/s) = \frac{3D\ distance}{transit\ time}$$

Distance traveled was measured in a 3D coordinate system combining the sagittal and axial imaging using at least 14 markers placed in the centerline of the aorta. The transit time was calculated using the least squares estimate between the systolic upslopes, which has shown to be most accurate and reproducible.(25,26) Measurements were repeated by another observer in 11 cases and showed excellent intra- and inter-observer reproducibility (ICC 0.99 and 0.95 respectively).

Local wave speed estimation

The central pressure waveform (P) was linearly interpolated to the same sample frequency as the ascending aorta velocity data (U), and waveforms were aligned using the foot and early part of the systolic upstroke in pressure and flow velocity (**Figure 1**). Alignment and analysis of physiological signals was performed using custom written software in Matlab R2016a (The MathWorks, Inc., Natick, Mass, USA). Based on the conservation of mass and momentum, wave speed, c , is a function of the change in pressure and velocity described by the water-hammer equation:(10)

$$dP_{\pm} = \pm \rho c dU_{\pm}$$

where + refers to waves moving away from the heart, – to waves moving towards the heart, and ρ is the density of blood (1050kg/m³).

It is assumed that reflected waves are absent in early systole, c was therefore estimated as the gradient of the PU-loop at this time, **Figure 2**:

$$c = \frac{1}{\rho} \frac{dP}{dU}$$

Wave speed can also be estimated by assuming that net wave energies are minimized over a complete cardiac cycle. This is known as the sum of squares method (cSS),(11) and was calculated as:

$$cSS = \frac{1}{\rho} \sqrt{\frac{\sum dP^2}{\sum dU^2}}$$

Wave intensity analysis

For WIA and *c*SS, the *P* and *U* waveforms were filtered using a standard 7 point, 2nd order polynomial Savitzky-Golay filter to smooth data and calculate derivatives.(27) Net wave intensity was calculated as the product of the derivative of pressure (*dP*) and velocity (*dU*) over the cardiac cycle:(9)

$$dI = dP \cdot dU$$

When wave speed is known (*c*), forward and backward wave intensity can be solved using the water-hammer equation:

$$WI_+ = \frac{1}{4\rho c} (dP + \rho c \cdot dU)^2$$
$$WI_- = -\frac{1}{4\rho c} (dP - \rho c \cdot dU)^2$$

where WI_+ is the forward wave intensity, WI_- is the backward wave intensity, and *c* is wave speed estimated using the PU-loop method.

Wave intensity was quantified using the magnitude and timing of the peak of three waves:(28) the initial forward compression (FCW), backward compression (BCW) and forward (protodiastolic) decompression (expansion) (FDW) waves (**Figure 1**). To enable comparisons between subjects, the sample period was normalised by the duration of the cardiac cycle,(15) but can be converted into W/m²/s² simply by multiplying by the heart rate per second. The reflection index was taken as the ratio of BCW/FCW.(17) Wave energy was calculated as the area under each wave. For comparison, wave separation analysis was performed to calculate the reflection magnitude, taken as the ratio of the backward to the forward wave amplitudes.(2)

Anthropomorphic and other assessments

Height was recorded using a standard stadiometer. Weight and body fat percentage were measured using digital bioimpedance scales (BC-418, Tanita, USA). Body surface area was calculated using the Mosteller formula. Maximal oxygen consumption (peak VO₂) was

estimated by a cardio-pulmonary exercise test (CPET) on a semi-supine ergometer (Ergoselect1200, Ergoline, Germany) using an incremental protocol standardized by bodyweight and gender, as previously described.(20)

Statistics

Data were analyzed in R (R foundation, Vienna, Austria) using RStudio Server version 0.98 (Boston, Mass, USA). All continuous variables are expressed as mean±SD or median(interquartile range,IQR) for skewed data. Normality was checked using the Shapiro-Wilk test. Categorical variables are expressed as percentages. Characteristics are stratified by age decile and gender. Groups were compared using independent-samples Student's t-tests for normally distributed continuous variables or Mann-Whitney U test and the Chi-square tests for non-normally distributed and categorical variables respectively. For trends over age deciles, the non-parametric Mann-Kendall monotonic trend test was used. Pearson's correlation coefficient (r) and Bland-Altman limits of agreement (LoA) were used to assess correlation and agreement respectively. Multivariable linear regression models for the association between age and WIA parameters were adjusted for covariates that a priori could confound the relationship; these were sex, heart rate, and height; similarly, sex was adjusted for age, heart rate and height. Mean arterial pressure was not included as it may be dependent on wave generation rather than the converse.(29) Regression diagnostics were performed and data were log-transformed if appropriate. All tests were two tailed, and $p < 0.05$ was considered statistically significant.

Results

Baseline characteristics

In 206 healthy volunteers, the median age was 37 years (range 21-73 years), 189 (92%) were normotensive (<140/90mmHg) on assessment; and mean aortic arch PWV_{tt} was 4.7±1.5m/s,

Table 1. The peak intensity of the initial compression wave, backward compression wave and forward decompression wave were 69.5±28, -6.6±4.2 and 6.2±2.5 x10⁴ W/m²/cycle² respectively; reflection index was 0.10±0.06.

Local wave speed compared to PWV_{tt}

There was a high degree of moderate correlation between PWV_{tt} and *c*, and this was stronger with *c*SS (*r*=0.60 and 0.68 respectively, *p*<0.01 for both). PWV_{tt} was greater than *c*, and this difference was reduced for *c*SS (difference:-1.3[LoA:-3.8 to 1.2] versus -0.64[LoA: -3.0 to 1.7]m/s respectively; **Figure 3**).

Wave speed and wave intensity by age decade

Both *c* and *c*SS increased from youngest (20-30 year-olds) to oldest (≥60 year-olds) age decade (**Figure 4**), although *c*SS tended to be higher than *c*. **Table 2** displays all WIA measures stratified by age decade and sex.

FCW decreased progressively with age up to 50-60 year-olds, but rose in ≥60 year-olds. The BCW increased steadily from youngest to oldest age decade. This resulted in a steady increase in reflection index with age decade. There was no convincing trend in FDW with age. Age-related trends were not modified by sex, so data for both sexes are pooled in **Figure 4**.

Associations of wave intensity after adjustment for potential confounders

In multivariable analysis including age, sex, heart rate and height as covariates, older age was associated with a smaller FCW, a larger BCW and a larger reflection index. Male sex was associated with a higher FCW, no difference in BCW and consequently a lower reflection

index, and a higher FDW compared with females. Higher heart rate was associated with a lower FCW, a lower BCW, a lower reflection index and a lower FDW. Height was not associated with any WIA parameter in adjusted models. Associations between WIA and peak VO₂, and body fat are detailed in Supplemental table 1 and Supplemental table 2.

Discussion

This is the first study to determine wave intensity and local wave speed by combining direct non-invasive measures of central blood pressure and velocity data from phase contrast cardiovascular magnetic resonance. This straightforward method allows aortic WIA to be performed at scale, here in the largest cohort reported to date. This technique was validated by showing good agreement between local wave speed (calculated from combined non-invasive pressure and phase contrast CMR-derived flow data) and conventionally measured pulse wave velocity using transit time. WIA patterns and magnitude appeared similar to invasive data,(13,30,31) but here the non-invasive nature of testing permitted exploration of healthy ventriculo-arterial coupling. The resolution was sufficient to detect that ageing and female sex were independently associated with decreased forward compression wave energy and an increased proportion of wave reflection, suggesting a less energy efficient cardiovascular system.

How can non-invasive aortic WIA be used?

A similar pattern of wave intensity was found in all individuals, which can help to improve our understanding of hemodynamics. We observed a dominant FCW in the early phase of LV ejection, which has been associated with myocardial contractility, and a smaller FDW, associated with the time constant of LV relaxation.(32) A BCW was also observed which is thought to relate to reflected late systolic afterload originating from distal sites of impedance mismatch.(31) These patterns and wave timings are similar to invasive studies, but an earlier BCW compared to other non-invasive data may reflect population characteristics or quantification differences (wave foot versus peak).(14,30,33)

Describing pressure and flow changes together, WIA has advanced the way we understand ventricular function and arterial coupling in different pathologies. Patients with chronic heart

failure have an impaired ability to generate a systolic FCW, but the FCW generated is reflected, increasing afterload.(34) Wave intensity can predict left ventricular ejection fraction recovery or quality of life improvement in patients undergoing valvular surgery, and help to identify sub-clinical systolic and diastolic dysfunction in children with heart failure and preserved ejection fraction.(35–37) Increased wave reflection is associated with outcomes in systemic hypertension,(4) aortic curvature, and in the pulmonary circulation is an early and specific marker in the development of pulmonary hypertension.(15,38,39) Due to reliance on invasive measures, most of these previous insights have been derived from studies of small patient cohorts. Non-invasive approaches have the potential to improve our understanding of cardiovascular hemodynamics in health and disease, and can be applied to longitudinal studies.

WIA at scale using central measures

Whilst central hemodynamics have most impact on the ventricle, previous non-invasive studies of WIA have typically been in peripheral arteries because they are easier to interrogate using ultrasound doppler and tonometry.(4,32) The approach developed in this study uses measures of central pressure and velocity rather than surrogates such as distensibility, which are dependent on aortic stiffness. Like other methods,(16) these were acquired sequentially, but simultaneous acquisition is feasible in future studies using longer tubing for the central blood pressure cuff measurement. This would enable the oscillometric device to be situated in the MRI control room for pressure measurement, whilst the patient has flow measured in the MRI scanner.

Local wave speed estimation

The validity of two single-point methods of wave speed were tested by comparing with a conventional regional estimate extending across the aortic arch (PWV_{tt}). (14) We used two previously described single-point methods, one based on the pressure-velocity loop,(10) and

the other using the sum-of-squares method.(11) Both showed acceptable agreement with the transit time based method which was assumed to be the reference, although agreement was slightly better for *cSS* which is consistent with the findings of a previous in-vitro study.(40) Because wave speed increases distally, both measures of ascending aortic local wave speed were expectedly lower than regional PWV_{tt} which extends to the aortic arch.

Associations between sex or age and aortic WIA

These data show that females have a greater wave reflection index in the aorta and lower FDW magnitude, which has not been reported previously, to our knowledge. Consistent with Li et al., females also demonstrated a smaller FCW.(14) Borlotti et al. found a sex difference in the reflection index in carotid but not femoral arteries, however wave reflection in the aorta is different to that seen in the carotid.(17) Differences in wave reflection may provide a substrate for the development of heart failure.(41)

The increase in wave speed and arterial stiffness with age are well recognized, however age-related changes in aortic WIA measures have only previously been described in one study, which used diameter rather than pressure measurements to derive an alternative index of wave intensity.(14) This study also reported a decrease in FCW, BCW and an increase in reflection index but reported a decrease in FDW rather than the lack of change seen in this study. Differences with these data may be due to different study populations, or the use of diameter as a surrogate measure of pressure in the previous study, which itself is inversely related to wave speed. The proportion of reflection increased with age whether measured by wave separation or wave intensity analysis. The contribution of higher intensity waves appears more pronounced at older ages and higher degrees of overall reflection. This suggests that the greater reflection that occurs with healthy ageing presents a more adverse load on the heart.(42)

Study limitations

Because data were acquired over several cardiac cycles and ensemble averaged, the average cycle is truncated leading to a slight shortening of the duration of diastole; however since wave intensity in end-diastole is negligibly small this is unlikely to affect our findings. Participants were recruited based on their intention to participate in a first marathon, and while they were not engaged in training at the time of study it is unlikely that they are representative of the general population. Older participants were relatively under represented and are probably biased through selective recruitment of more healthy individuals. Similarly, patients were excluded with any known significant medical problems including hypertension or diabetes mellitus. We used a free-breathing phase-contrast CMR sequence which provides sufficient spatio-temporal resolution for the velocity profile. A similar sequence has also been used to measure CMR distensibility as a surrogate for central pressure, but because it is free-breathing this may compromise accuracy for measures of compliance due to through-plane motion.(33) Breath-held sequences are possible using an accelerated spiral sequence but can be difficult to analyze due to respiratory artifact or lower signal to noise.(43) Hematocrit differences between sexes were not accounted for, although this is unlikely to affect blood density significantly.

Conclusion

This paper describes a novel non-invasive method for wave intensity analysis, using central blood pressure and CMR velocity data. Local wave speed measured by this technique showed good agreement with regional pulse wave velocity and the method has straightforward application for large sample sizes. In healthy individuals, women had a smaller forward compression wave, and poorer overall ventriculo-arterial coupling than men. In both sexes, older age was associated with higher wave speed and poorer ventriculo-arterial coupling as assessed by WIA.

Acknowledgements

The study was jointly funded by the British Heart Foundation (FS/15/27/31465), Cardiac Risk in the Young and the Barts Cardiovascular Biomedical Research Centre. The study received support from COSMED (Rome, Italy) through the provision of cardiopulmonary exercise testing equipment and technical support.

We thank the study participants for their time and taking part in the study. We are also grateful to Virgin London Marathon for their support in recruitment of participants. We are grateful to the entire marathon study team performing investigations. In addition to the authors of this manuscript, The Marathon Study group included the following staff from St George's University of London, University College London, Bart's Health Trust and other organisations: Andrew D'Silva, Camilla Torlasco, Anish Bhuvu, Siana Jones, Jet Van Zalen, Amna Abdel-Gadir, Thomas Treibel, Stefania Rosmini, Manish Ramlall, Gabriella Captur, Katia D Menacho Medina, Joao Augusto, Yang Ye, Niromila Nadarajan, Nabila Mughul, Sunita Chauhan, Shino Kirokose, Tolu Akinola, Cheelo Simaanya, Lizette Cash, James Willis, David Hoare, James Malcolmson, Pamela de la Cruz, Annabelle Freeman, Delfin Encarnacion, Lesley Hart, Jack Kaufman, Frances Price, Rueben Dane, Karen Armado, Gemma Cruz, Lorna Carby, Tiago Fonseca, Fatima Niones, Zeph Fanton, Jim Pate, Joe Carlton, Sarah Anderson, Rob Hall, Sam Liu, Sonia Bains, Claire Kirkby, Pushpinder Kalra, Raghuveer Singh, Bode Ensam, Tee J Yeo, Rachel Bastiaenen, Della Cole, Jacky Ah- Fong, Sue Brown, Sarah Horan, Ailsa McClean, Kyle Conley, Paul Scully, Luke Horsfield, Mark McLaren, Elizabeth Clough, Daniel Key, Riyaz Patel and Sanjeev Bhattacharyya. We are grateful to Virgin Money London Marathon, particularly Hugh Brasher and Penny Dain, for their support with study advertisement and participant recruitment. From our funders Cardiac Risk in the Young we are particularly grateful to Steve Cox and Azra Loncarevic-Srmic for their additional support with administration and transport.

References

1. Mitchell GF, Tardif J-C, Arnold JMO, Marchiori G, O'Brien TX, Dunlap ME, et al. Pulsatile Hemodynamics in Congestive Heart Failure. *Hypertension*. 2001;38(6):1433–9.
2. Parker K, Jones CJ. Forward and Backward Running Waves in the Arteries: Analysis Using the Method of Characteristics. *J Biomech Eng*. 1990;112:322–6.
3. London GM, Blacher J, Pannier B, Guérin AP, Marchais SJ, Safar ME. Arterial Wave Reflections and Survival in End-Stage Renal Failure. *Hypertension*. 2001;38(3):434–84.
4. Manisty C, Mayet J, Tapp RJ, Parker KH, Sever P, Poulter NH, et al. Wave Reflection Predicts Cardiovascular Events in Hypertensive Individuals Independent of Blood Pressure and Other Cardiovascular Risk Factors: An ASCOT Substudy. *J Am Coll Cardiol*. 2010;56(1):24–30.
5. Laurent S, Boutouyrie P, Asmar R, Gautier I, Laloux B, Guize L, et al. Aortic stiffness is an independent predictor of all-cause and cardiovascular mortality in hypertensive patients. *Hypertension*. 2001;37(5):1236–41.
6. Sen S, Escaned J, Malik IS, Mikhail GW, Foale RA, Mila R, et al. Development and Validation of a New Adenosine-Independent Index of Stenosis Severity From Coronary Wave–Intensity Analysis. *J Am Coll Cardiol*. 2012 Apr 10;59(15):1392–402.
7. Laurent S, Cockcroft J, Van Bortel L, Boutouyrie P, Giannattasio C, Hayoz D, et al. Expert consensus document on arterial stiffness: Methodological issues and clinical applications. *Eur Heart J*. 2006;27(21):2588–605.
8. Ben-Shlomo Y, Spears M, Boustred C, May M, Anderson SG, Benjamin EJ, et al. Aortic pulse wave velocity improves cardiovascular event prediction: An individual participant meta-analysis of prospective observational data from 17,635 subjects. *J Am Coll Cardiol*. 2014;63(7):636–46.

9. Parker KH. An introduction to wave intensity analysis. *Med Biol Eng Comput.* 2009;47(2):175–88.
10. Khir AW, O'Brien A, Gibbs JS, Parker KH. Determination of wave speed and wave separation in the arteries. *J Biomech.* 2001 Sep;34(9):1145–55.
11. Davies JE. Use of simultaneous pressure and velocity measurements to estimate arterial wave speed at a single site in humans. *AJP Hear Circ Physiol.* 2005;290(2):H878–85.
12. Segers P, Swillens A, Taelman L, Vierendeels J. Wave reflection leads to over- and underestimation of local wave speed by the PU- and QA-loop methods: Theoretical basis and solution to the problem. *Physiol Meas.* 2014;35(5):847–61.
13. Koh TW, Pepper JR, Desouza AC, Parker KH. Analysis of wave reflections in the arterial system using wave intensity: A novel method for predicting the timing and amplitude of reflected waves. *Heart Vessels.* 1998;13(3):103–13.
14. Li Y, Hickson SS, McEniery CM, Wilkinson IB, Khir AW. Stiffening and ventricular–arterial interaction in the ascending aorta using MRI. *J Hypertens.* 2019; 37(2):347-355.
15. Su J, Manisty C, Parker KH, Simonsen U, Nielsen-Kudsk JE, Mellekjaer S, et al. Wave Intensity Analysis Provides Novel Insights Into Pulmonary Arterial Hypertension and Chronic Thromboembolic Pulmonary Hypertension. *J Am Heart Assoc.* 2017;6(11).
16. Zambanini A. Wave-energy patterns in carotid, brachial, and radial arteries: a noninvasive approach using wave-intensity analysis. *AJP Hear Circ Physiol/* 2005;289(1):H270–6.
17. Borlotti A, Khir AW, Rietzschel ER, De Buyzere ML, Vermeersch S, Segers P. Noninvasive determination of local pulse wave velocity and wave intensity: changes with age and gender in the carotid and femoral arteries of healthy human. *J Appl Physiol.* 2012;113(5):727–35.

18. Quail MA, Steeden JA, Knight D, Segers P, Taylor AM, Muthurangu V. Development and validation of a novel method to derive central aortic systolic pressure from the MR aortic distension curve. *J Magn Reson Imaging*. 2014;40(5):1064–70.
19. Park CM, Korolkova O, Davies JE, Parker KH, Siggers JH, March K, et al. Arterial pressure: agreement between a brachial cuff-based device and radial tonometry. *J Hypertens*. 2014;32(4):865–72.
20. Jones S, D’Silva A, Bhuvu A, Lloyd G, Manisty C, Moon JC, et al. Improved exercise-related skeletal muscle oxygen consumption following uptake of endurance training measured using near-infrared spectroscopy. *Front Physiol*. 2017;8(12):1–8.
21. Lin ACW, Lowe A, Sidhu K, Harrison W, Ruygrok P, Stewart R. Evaluation of a novel sphygmomanometer, which estimates central aortic blood pressure from analysis of brachial artery suprasystolic pressure waves. *J Hypertens*. 2012;30(9):1743–50.
22. Climie RED, Schultz MG, Nikolic SB, Ahuja KDK, Fell JW, Sharman JE. Validity and reliability of central blood pressure estimated by upper arm oscillometric cuff pressure. *Am J Hypertens*. 2012;25(4):414–20.
23. De Cesare A, Redheuil A, Dogui A, Engineer O, Lalande A, Frouin F, et al. ART-FUN: an integrated software for functional analysis of the aorta. *J Cardiovasc Magn Reson*. 2009;11(Suppl 1):P182.
24. Herment A, Kachenoura N, Lefort M, Bensalah M, Dogui A, Frouin F, et al. Automated segmentation of the aorta from phase contrast MR images: Validation against expert tracing in healthy volunteers and in patients with a dilated aorta. *J Magn Reson Imaging*. 2010;31(4):881–8.
25. Dogui A, Redheuil A, Lefort M, DeCesare A, Kachenoura N, Herment A, et al. Measurement of aortic arch pulse wave velocity in cardiovascular MR: Comparison of transit

time estimators and description of a new approach. *J Magn Reson Imaging*.

2011;33(6):1321–9.

26. Redheuil A, Yu W-C, Wu CO, Mousseaux E, de Cesare A, Yan R, et al. Reduced ascending aortic strain and distensibility: earliest manifestations of vascular aging in humans.

Hypertens. 2010;55(2):319–26.

27. Savitzky A, Golay MJE. Smoothing and Differentiation of Data by Simplified Least Squares Procedures. *Anal Chem*. 1964;36(8):1627–39.

28. Parker KH, Jones CJH, Dawson JR, Gibson DG. What stops the flow of blood from the heart? *Heart Vessel*. 1988;(4):241–5.

29. Hughes AD, Davies JE, Parker KH. The importance of wave reflection: A comparison of wave intensity analysis and separation of pressure into forward and backward components.

Conf Proc IEEE Eng Med Biol Soc. 2013;2013:229–32.

30. Davies JE, Alastruey J, Francis DP, Hadjiloizou N, Whinnett ZI, Manisty CH, et al. Attenuation of Wave Reflection by Wave Entrapment Creates a “Horizon Effect” in the Human Aorta.

Hypertension. 2012;60(3):778–85.

31. Hughes AD, Parker KH, Davies JE. Waves in arteries: A review of wave intensity analysis in the systemic and coronary circulations. *Artery Res*. 2008;2(2):51–9.

32. Ohte N, Narita H, Sugawara M, Niki K, Okada T, Harada A, et al. Clinical usefulness of carotid arterial wave intensity in assessing left ventricular systolic and early diastolic performance.

Heart Vessels. 2003;18(3):107–11.

33. Li Y, Borlotti A, Hickson SS, McEniery CM, Wilkinson IB, Khir AW. Using magnetic resonance imaging measurements for the determination of local wave speed and arrival time of reflected waves in human ascending aorta. *Conf Proc IEEE Eng Med Biol Soc*. 2010;5153–6.

34. Curtis SL, Zambanini A, Mayet J, McG Thom SA, Foale R, Parker KH, et al. Reduced systolic wave generation and increased peripheral wave reflection in chronic heart failure. *AJP Hear Circ Physiol*. 2007;293(1):H557–62.
35. Ntsinjana HN, Chung R, Ciliberti P, Muthurangu V, Schievano S, Marek J, et al. Utility of Cardiovascular Magnetic Resonance-Derived Wave Intensity Analysis As a Marker of Ventricular Function in Children with Heart Failure and Normal Ejection Fraction. *Front Pediatr*. 2017 Apr 3; 5:65.
36. Niki K, Sugawara M, Kayanuma H, Takamisawa I, Watanabe H, Mahara K, et al. Associations of increased arterial stiffness with left ventricular ejection performance and right ventricular systolic pressure in mitral regurgitation before and after surgery: Wave intensity analysis. *Int J Cardiol Hear Vasc*. 2017;16:7–13.
37. Chirinos JA, Akers SR, Schelbert E, Snyder BS, Witschey WR, Jacob RM, et al. Arterial Properties as Determinants of Left Ventricular Mass and Fibrosis in Severe Aortic Stenosis: Findings From ACRIN PA 4008. *J Am Heart Assoc*. 2019 Jan 8;8(1):e03742.
38. Quail MA, Knight DS, Steeden JA, Taelman L, Moledina S, Taylor AM, et al. Noninvasive pulmonary artery wave intensity analysis in pulmonary hypertension. *Am J Physiol Circ Physiol*. 2015 Jun 15;308(12):H1603–11.
39. Quail MA, Segers P, Steeden JA, Muthurangu V. The aorta after coarctation repair - effects of calibre and curvature on arterial haemodynamics. *J Cardiovasc Magn Reson*. 2019 Apr 11;21(1):22.
40. Aguado-Sierra J, Parker KH, Davies JE, Francis D, Hughes AD, Mayet J. Arterial pulse wave velocity in coronary arteries. In: 2006 International Conference of the IEEE Engineering in Medicine and Biology Society. IEEE; 2006. p. 867–70.
41. Weber T, Chirinos JA. Pulsatile arterial haemodynamics in heart failure. *Eur Heart J*. 2018 Jun 26;39(43):3847–54.

42. Phan TS, Li JK-J, Segers P, Reddy-Koppula M, Akers SR, Kuna ST, et al. Aging is Associated With an Earlier Arrival of Reflected Waves Without a Distal Shift in Reflection Sites. *J Am Heart Assoc.* 2016;5(9).
43. Biglino G, Steeden JA, Baker C, Schievano S, Taylor AM, Parker KH, et al. A non invasive clinical application of wave intensity analysis based on ultrahigh temporal resolution phase-contrast cardiovascular magnetic resonance. *J Cardiovasc Magn Reson.* 2012 Jan 9;14(1):57.

Table legends

Table 1 Study participant characteristics stratified by sex and age decile.

Table 2 Wave intensity analysis stratified by sex and age decile.

Participant characteristics	Males					Females				
	20-30	30-40	40-50	50-60	60+	20-30	30-40	40-50	50-60	60+
<i>n</i>	31	31	22	9	3	33	35	30	9	3
Age/ years	26 ±2	32 ±2	44 ±3	54 ±2	66 ±4	26 ±2	33 ±3	45 ±3	54 ±2	67 ±6
Height/ cm	181 ±7	181 ±7	180 ±6	177 ±9	172 ±4	167 ±5	167 ±5	167 ±6	169 ±5	160 ±5
Weight/ kg	78 ±8	82 ±15	85 ±9	81 ±15	76 ±7	63 ±9	69 ±11	69 ±15	71 ±13	70 ±16
BMI/ kg.m ⁻²	24 ±3	25 ±4	26 ±3	26 ±4	26 ±2	22 ±3	25 ±4	25 ±5	25 ±5	27 ±5
BSA/ m ²	2.0 ±0.1	2.0 ±0.2	2.0 ±0.1	2.0 ±0.2	1.9 ±0.1	1.7 ±0.1	1.8 ±0.1	1.8 ±0.2	1.8 ±0.1	1.7 ±0.2
Body Fat/ %	15 ±5	20 ±6	23 ±5	22 ±6	23 ±2	28 ±6	32 ±7	32 ±8	33 ±8	35 ±7
Peak VO ₂ / ml/kg/min	43 ±6	38 ±6	33 ±6	34 ±7	25 ±3	35 ±4	32 ±6	29 ±7	24 ±4	24 ±3
Resting Heart Rate/ bpm	70 ±15	70 ±15	72 ±14	67 ±14	64 ±4	74 ±15	71 ±10	69 ±12	67 ±12	67 ±11
Brachial SBP/ mmHg	124 ±11	124 ±12	128 ±10	133 ±18	146 ±19	113 ±8	113 ±10	117 ±13	127 ±20	136 ±33
Brachial DBP/ mmHg	75 ±4	75 ±6	79 ±5	79 ±7	79 ±10	72 ±5	73 ±6	74 ±7	80 ±10	76 ±18
Aortic SBP/ mmHg	113 ±10	113 ±10	117 ±9	124 ±19	136 ±23	104 ±8	106 ±10	109 ±11	122 ±19	129 ±31

Table 1 Study participant characteristics stratified by sex and age decile. Abbreviations: BMI: body mass index; BSA: body surface area; DBP: diastolic blood pressure; MAP: mean arterial pressure; SBP: systolic blood pressure; peak V02: maximal oxygen consumption.

Wave intensity measures	Males					Females								
	20-30	30-40	40-50	50-60	60+	20-30	30-40	40-50	50-60	60+				
Wave speed/ ms⁻¹														
<i>c</i>	3.4 ±0.9	3.3 ±1.1	3.9 ±1.2	4.9 ±2.0	5.7 ±1.8	2.7 ±0.6	2.7 ±0.8	3.3 ±1.0	4.0 ±1.0	5.2 ±2.9				
<i>cSS</i>	3.4 ±0.9	3.6 ±0.9	4.6 ±1.2	5.8 ±2.3	7.3 ±2.4	3.0 ±0.7	3.5 ±0.8	4.3 ±1.1	5.5 ±2.0	7.3 ±4.2				
Pulse wave velocity/ m/s	4 ±0.7	4 ±0.7	5 ±1.1	7 ±1.8	9 ±3.4	4 ±0.6	4 ±0.6	5 ±0.9	8 ±2.1	7 ±1.6				
Wave peak/ 10⁴ W/m²/cycle²														
FCW	99 ±35	84 ±27	61 ±23	62 ±17	71 ±1	67 ±22	61 ±24	52 ±14	47 ±9	68 ±19				
BCW	7.0 ±4	5.9 ±3	6.1 ±4	8 ±5	11.6 ±6	5.3 ±5	6.0 ±4	7.4 ±5	7.7 ±5	10.5 ±3				
FDW	8.4 ±3	6.7 ±2	6.2 ±2	7.5 ±3	10.3 ±3	5.2 ±2	4.8 ±2	5.2 ±2	6.5 ±1	6.6 ±2				
Wave timing/ ms														
FCW	50 ±5	50 ±7	52 ±4	53 ±3	56 ±3	49 ±5	48 ±4	51 ±5	53 ±2	53 ±2				
BCW	152 ±32	163 ±24	169 ±14	164 ±11	162 ±8	158 ±19	154 ±28	157 ±32	167 ±8	164 ±6				
FDW	258 ±38	268 ±40	275 ±26	303 ±48	303 ±19	272 ±40	272 ±45	296 ±27	311 ±25	306 ±33				
Reflection index	0.06 ±0.03	0.07 ±0.02	0.10 ±0.04	0.12 ±0.05	0.16 ±0.08	0.07 ±0.05	0.10 ±0.07	0.14 ±0.07	0.17 ±0.11	0.16 ±0.03				
Reflection magnitude	0.54 ±0.1	0.55 ±0.1	0.58 ±0.1	0.56 ±0.1	0.59 ±0.1	0.55 ±0.1	0.57 ±0.1	0.61 ±0.1	0.59 ±0.1	0.61 ±0.1				
Wave energy/ J														
Forward wave	5.6 ±1.6	4.6 ±1.4	3.6 ±1.0	3.5 ±0.7	4.6 ±0.5	3.5 ±1.1	3.5 ±1.2	3.0 ±0.6	2.9 ±0.4	4.3 ±1.0				
Backward wave	0.74 ±0.4	0.67 ±0.2	0.65 ±0.3	0.70 ±0.4	1.05 ±0.4	0.58 ±0.4	0.67 ±0.3	0.71 ±0.4	0.73 ±0.3	1.13 ±0.4				

Table 2 Wave intensity analysis stratified by sex and age decile. Pulse wave velocity was measured conventionally in the aortic arch from transit time. *Abbreviations: c: wave speed measured by the pressure-velocity loop; cSS: wave speed measured by the sum of squares method; BCW: backward compression wave; FCW: forward compression wave; FDW: forward decompression wave; J: joules.*

Figure legends

Figure 1 Aortic wave intensity analysis. Top: Foot-to-foot alignment of scaled pressure (blue) and velocity (red) waveforms. **Bottom:** Wave intensity analysis example showing initial compression (FCW), backward compression (BCW) and protodiastolic decompression (FDW) waves.

Figure 2 Analysis of blood pressure and CMR-derived velocity data. (A) After a period of rest the patient underwent oscillometric brachial blood pressure on two occasions immediately prior to MRI. A Pulsecor BP+ device acquired 10s of brachial waveforms at 200Hz. After, phase-contrast MRI was acquired at the level of the pulmonary artery using a free-breathing ECG gated sequence, acquired at c.100Hz at 60bpm. **(B)** A single ensemble averaged central pressure (P) was estimated and velocity (U) measured at each time point. **(C)** Data was aligned by waveform foot to foot. **(D)** wave speed measured in early systole using the pressure-velocity loop and sum of squares method after the application of a Savitsky-Golay filter. **(E)** Wave intensity calculated using the derivatives of pressure and velocity. ρ : density of blood (1050kg/m^3), c : P-U derived wave speed; cSS : sum of squares estimated c .

Figure 3 Correlation (top row) and Bland- Altman analysis (bottom row) of wave speed and pulse wave velocity (PWV) measured by transit time. Left: wave speed calculated from the pressure-velocity slope during early systole (c) **Right:** wave speed calculated from the sum of squares method (cSS).

Figure 4 Influence of age on wave speed and wave intensity indices. (A) wave speed (c) measured by PU-loop. **(B)** wave speed measured by sum of squares method (cSS). **(C)** Forward compression wave. **(D)** Backward compression wave. **(E)** Forward decompression wave. **(F)** Reflection index. *Abbreviations: ns: $p > 0.05$, * $p < 0.05$, **** $p < 0.0001$.*

Figure 1 Pressure and flow alignment to calculate wave intensities

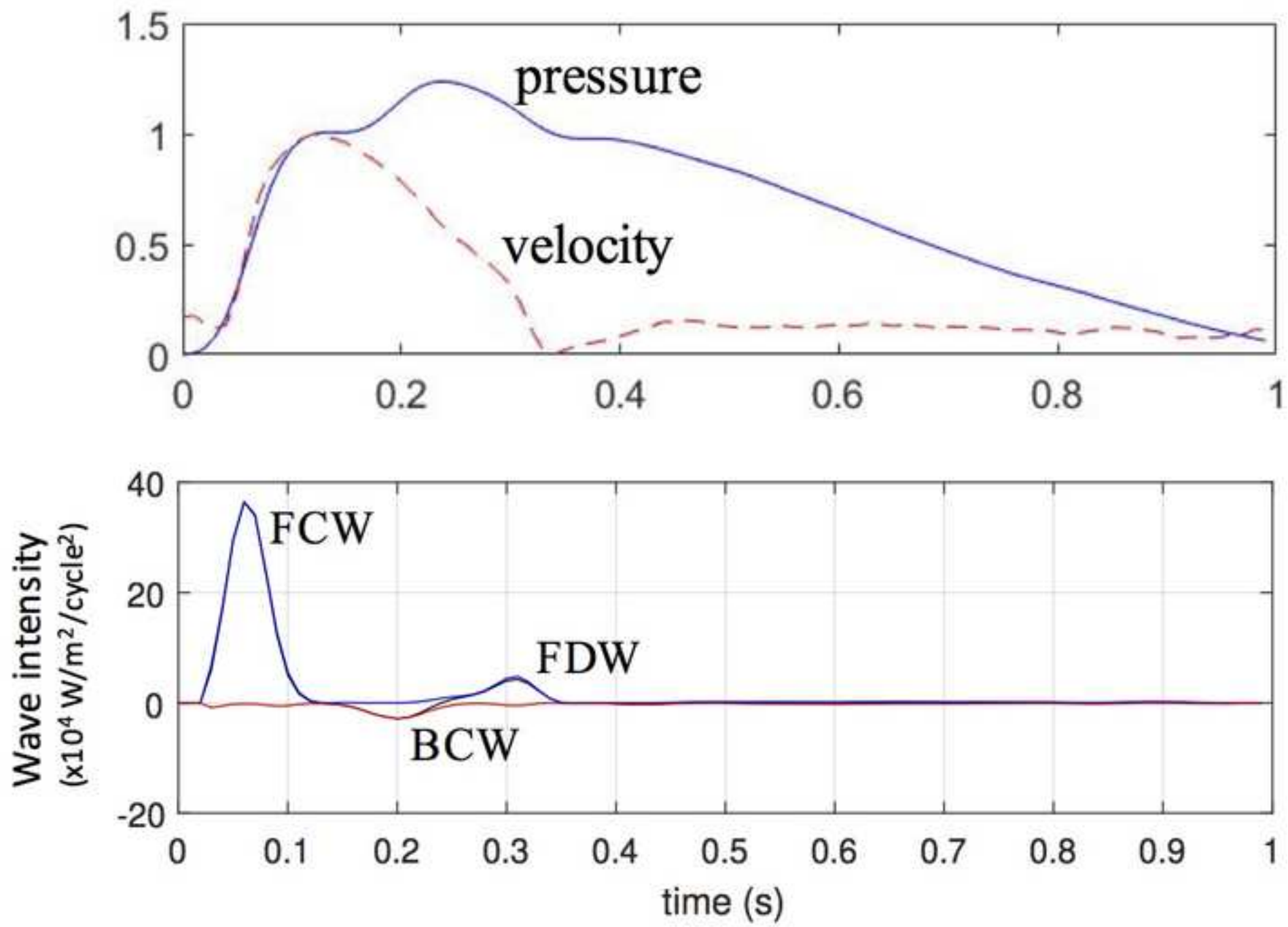


Figure 2 Wave intensity analysis methodology

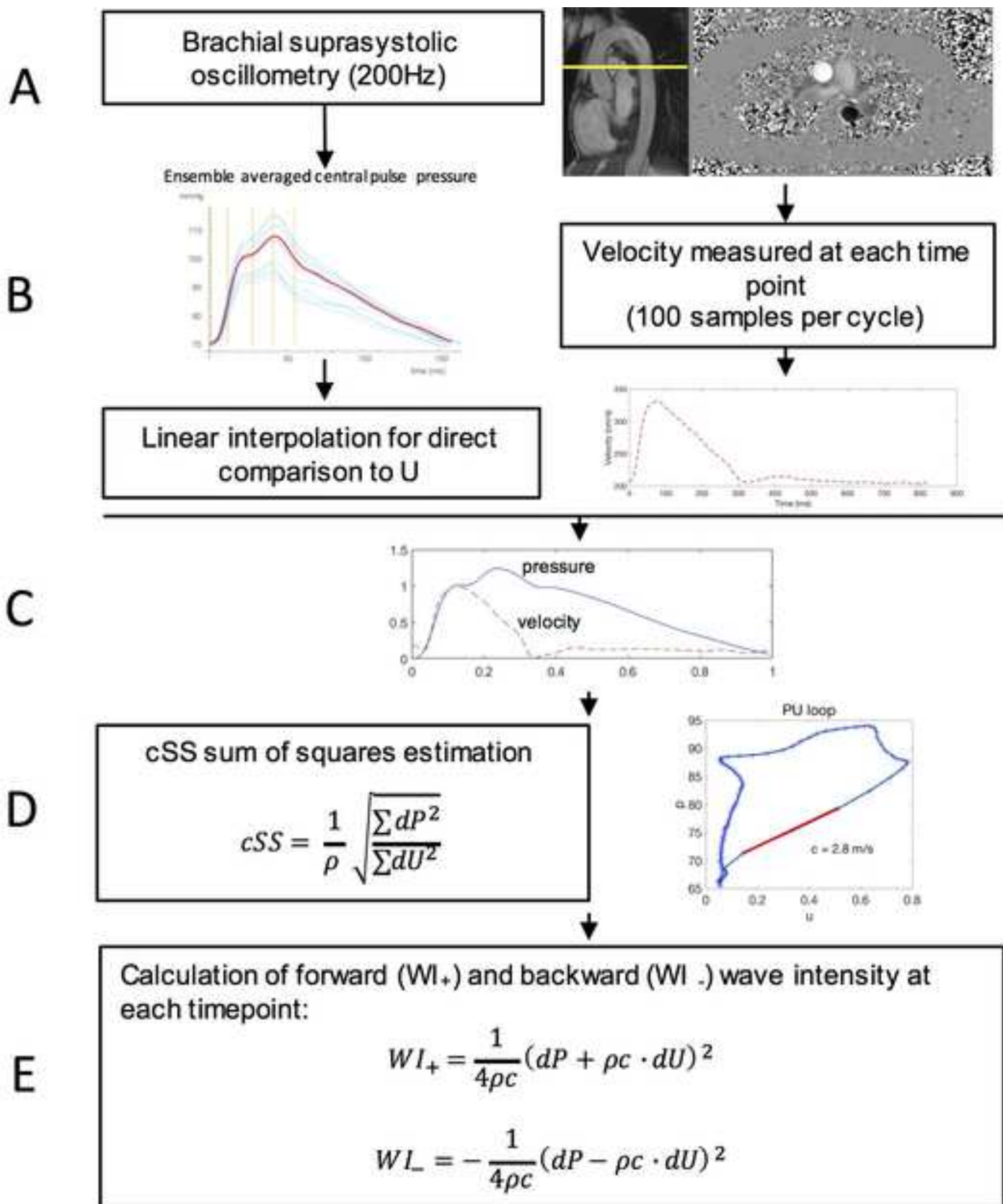


Figure 3 Local wave speed compared to regional pulse velocity is better for sum of squares than pressure velocity method

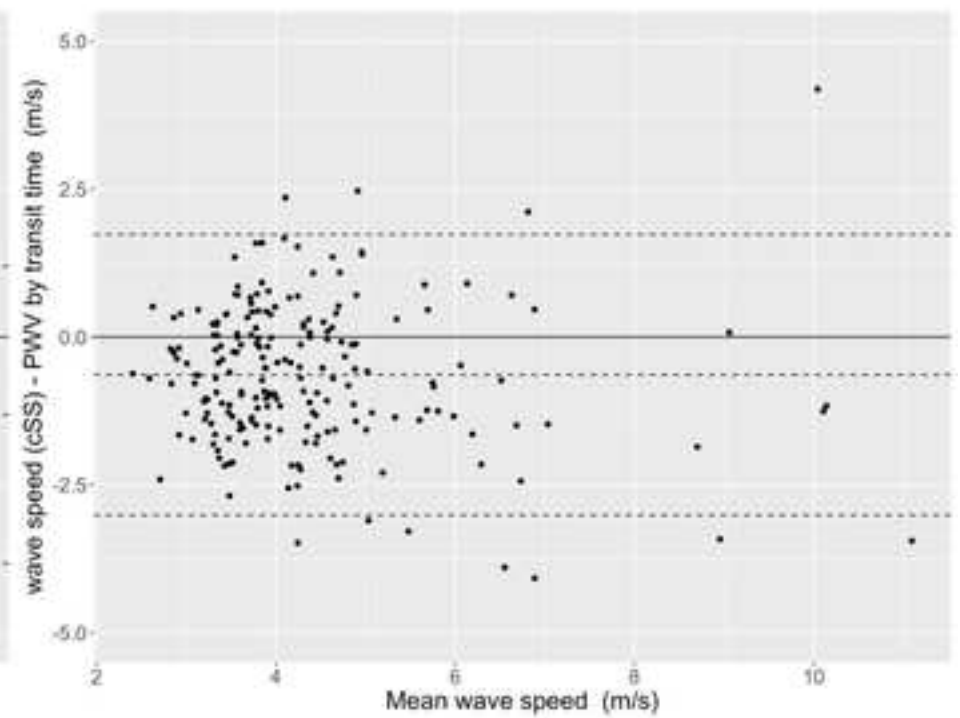
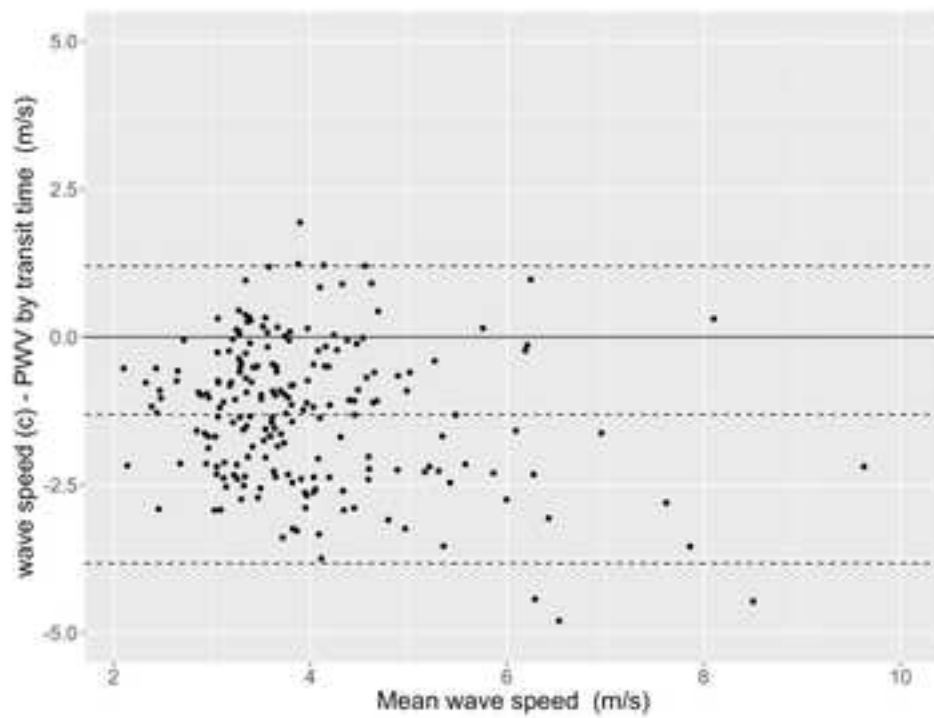
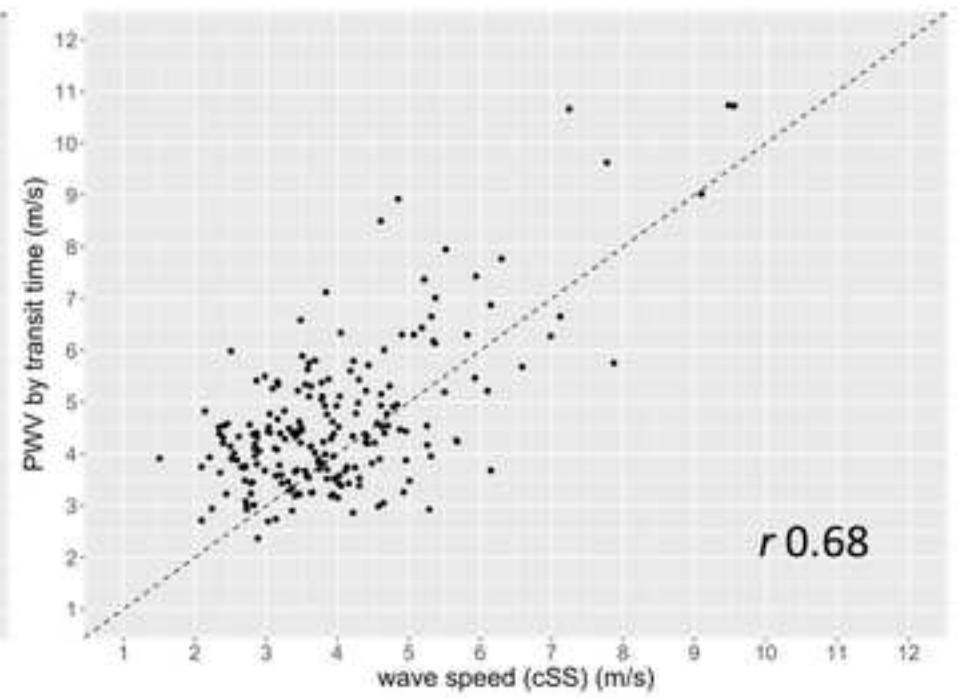
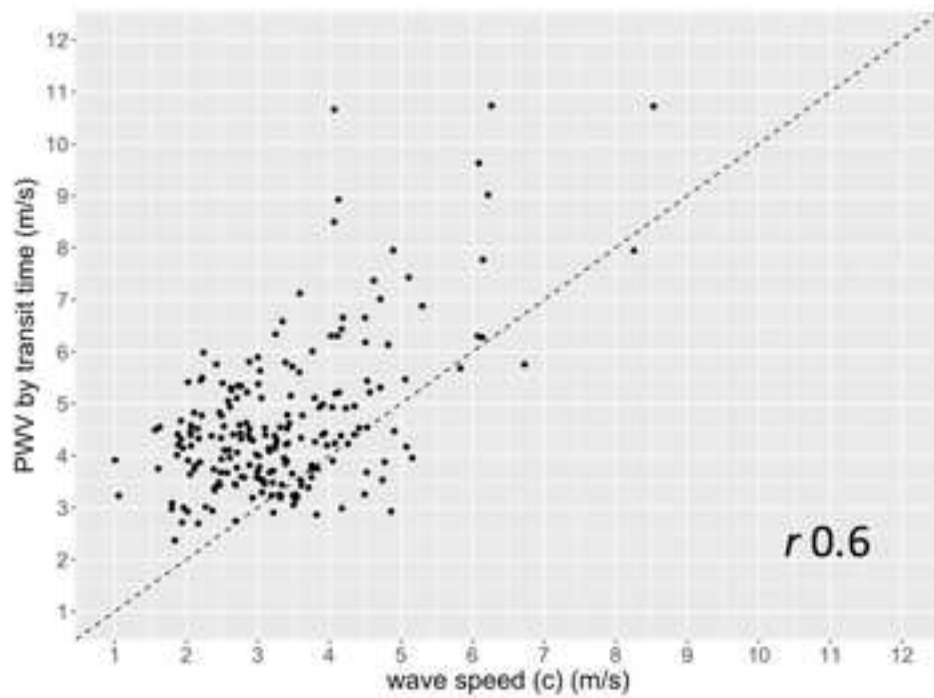


Figure 4 Influence of age on wave speed and wave intensity indices

